# EXPERIMENTAL NUCLEONICS

BY

ERNST BLEULER

*Professor of Physics*
*Purdue University*

AND

GEORGE J. GOLDSMITH

*Instructor in Physics*
*Purdue University*

RINEHART & COMPANY, INC., NEW YORK

EXPERIMENT **19** *Range and Energy Loss of Alpha Particles*

Range measurements may be used for the determination of the energy of heavy particles. Although the method cannot compete in accuracy with energy measurements by magnetic or electric deflection, it has the advantage of being comparatively simple and versatile. It is (or has been) used for the investigation of the natural alpha-ray spectra; the $Q$ values of nuclear reactions—giving information on nuclear masses and excited states of nuclei; the energy distribution and nature of cosmic rays; and the production and decay of mesons. The ranges are measured in the gas of a cloud chamber; by absorption (e.g., in aluminum), using a proportional counter or a shallow ionization chamber as a detector; or in the photographic plate.

Knowledge of the energy loss in different materials is necessary for the evaluation of corrections due to finite target or source thickness. Furthermore, since the construction of high-energy accelerators, it has become of increasing practical interest with respect to shielding problems. Although work with natural alpha particles is harmless because they are stopped in the skin, heavy shielding is necessary from alpha particles accelerated in these high-energy machines. For example, alpha particles of 400 Mev penetrate 3.6 cm of aluminum or 1.4 cm of lead.

In the experiment, the range of Po alpha partides in air and the stopping power of different metals are measured.

## ENERGY LOSS AND RANGE OF ALPHA PARTICLES IN AIR[1,2]

### *RATE OF ENERGY LOSS*

If a heavy particle—appreciably heavier than the electron—of mass $M$ and charge $ze$ moves with a velocity $v$ through a medium containing $N$

atoms of charge number $\mathcal{Z}$ per cm³, it loses its kinetic energy by ionization and excitation at a rate

$$-\frac{dE}{dx} = \frac{4\pi e^4 z^2}{mv^2} NB \tag{19.1}$$

with

$$B = \mathcal{Z} \ln \frac{2mv^2}{I} \tag{19.2}$$

$m$ being the rest mass of the electron, $B$ the stopping number of the (stopping) atom, and $I$ its average excitation potential. For air, the value of $I$ is determined experimentally to be 80.5 ev if an average value of $\mathcal{Z} = 7.22$ is assumed.

Figure 19.1 shows $-\frac{dE}{dx}$ in air for alpha particles and protons as a function of their energy. The central part of the curve (5 Mev $< E_\alpha <$ 500 Mev) is well represented by equations 19.1, 2. The prominent feature is the decrease of energy loss with increasing energy. At relativistic velocities, however, it does not reach an asymptotic value as expected but rises again. This is expressed by a correction term in $B$:

$$B = \mathcal{Z}\left[\ln \frac{2mv^2}{I} - \ln\left(1 - \frac{v^2}{c^2}\right) - \frac{v^2}{c^2}\right] \tag{19.3}$$

At low velocities, on the other hand, equation 19.2 fails because it is valid only as long as the velocities of all orbital electrons are small compared to the velocity of the incident particle. In the case of alpha particles of a few Mev, this condition is not fulfilled for the $K$ electrons of air. These contribute less to the stopping power, so that an energy dependent correction $C_k$ must be subtracted from the stopping number $B$ given in equation 19.2:[1]

$$B = \mathcal{Z} \ln \frac{2mv^2}{I} - C_k(v) \tag{19.4}$$

At still lower energies, the alpha particle may capture temporarily one or two electrons and become partly or fully neutralized. The energy loss is decreased. This effect is important when the alpha particle moves with a speed comparable to the orbital velocity of the He $K$ electrons. The influence of temporary neutralization is less in the case of the proton as is evident from the difference in the rate of energy loss at low velocities (cf. Figure 19.1).



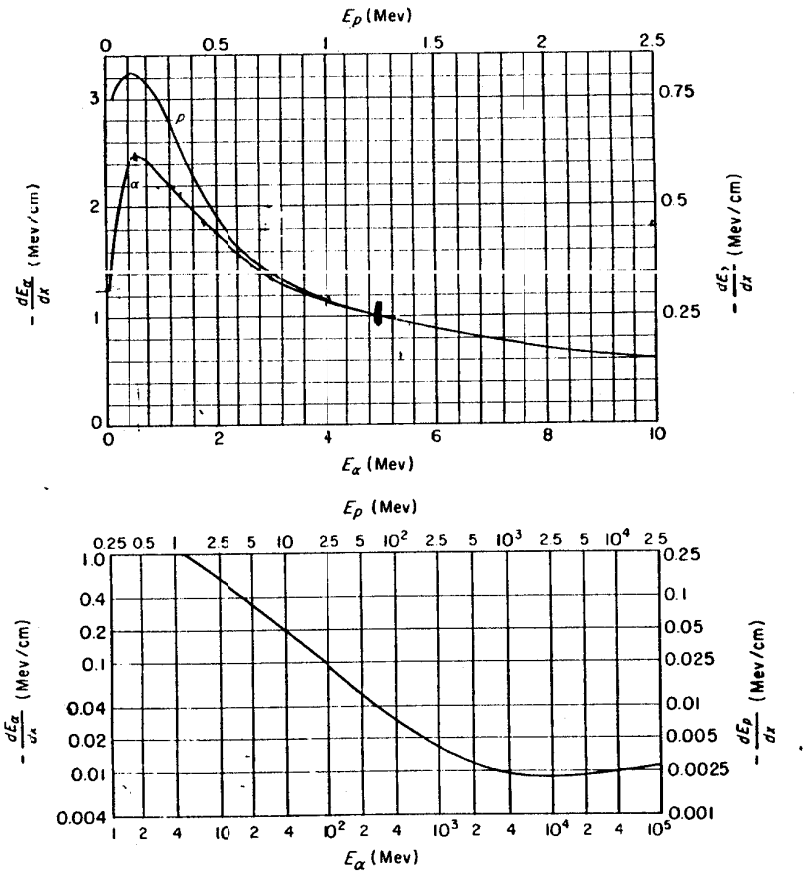


Fig. 19.1. Rate of energy loss in air of 1.226 mg/cm³ density for alpha particles and protons.[2]

*BRAGG CURVE*

The factor $\frac{dE}{dx}$ can be determined approximately by measuring the ionization in a shallow ionization chamber for different positions along

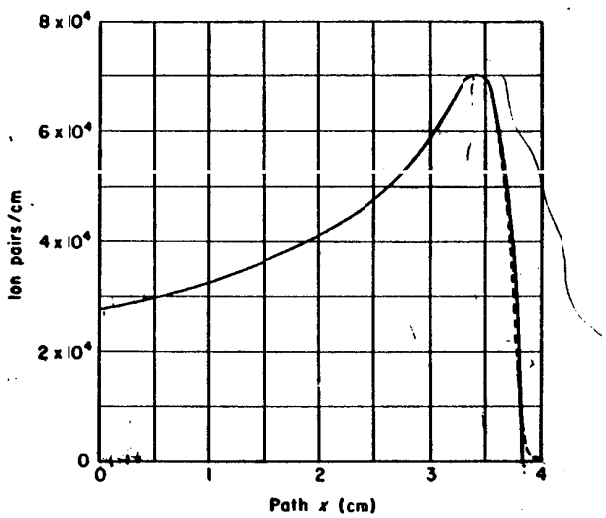


Fig. 19.2. Ionization-distance curve for Po alpha particles. —— single particle (a). - - - average for collimated beam, Bragg curve (b).

the path of the particle.[3] The number $n$ of ion pairs formed per unit path length is related to the energy loss

$$n = -\frac{dE}{dx}\frac{1}{\epsilon} \tag{19.5}$$

where $\epsilon$ is the mean energy spent per ion pair. It appears to be constant over a large range of energies—~ 32.5 ev per ion pair in air—rising only at very low velocities. Figure 19.2 shows the single-particle ionization curve (a) for a Po alpha particle which stops at $x = 3.84$ cm. Since the distances traveled by different alpha particles are not exactly identical (see below), the average ionization curve measured for a collimated beam of alpha particles differs slightly from (a). It is called the Bragg curve (b). The single-particle curve can be calculated from the measured Bragg curve if the amount of range straggling is known.



*MEAN RANGE OF ALPHA PARTICLES*

The range of an alpha particle is that path length after which it has lost the whole initial energy $E$.

$$R = \int_0^E \frac{dE'}{-dE'/dx} \tag{19.6}$$

For a source of monokinetic alpha particles, the ranges of the individual particles are not exactly equal because of statistical fluctuations of the

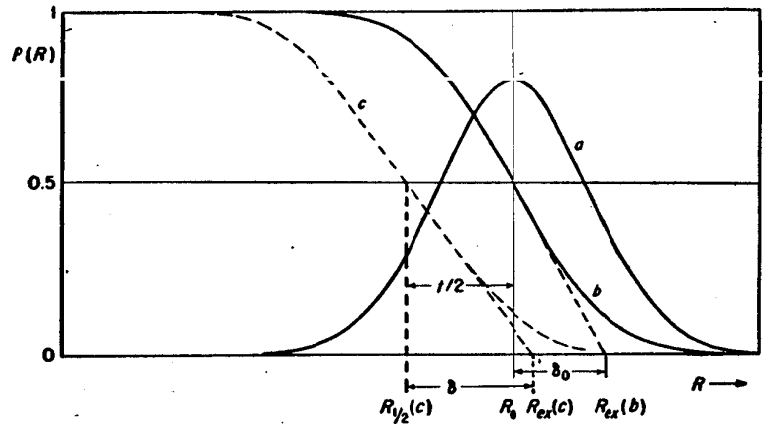


Fig. 19.3. Range distributions for alpha particles of mean range $R_0$. a = differential range distribution, $p(R)$, for thin source. b = integral range distribution, $P(R)$, for thin source. c = integral range distribution for source of finite thickness $t$. Note that the extrapolated range of curve c is very close to the true mean range $R_0$.

energy loss. They straggle about an average value, the mean range. The distribution of track lengths, as measured in a cloud chamber, can be represented by a Gaussian curve (see Figure 19.3, curve *a*):

$$p(R) = \frac{\alpha}{\sqrt{\pi}} e^{-\alpha^2(R-R_0)^2} \tag{19.7}$$

$\alpha$ being called the straggling parameter.

Most counting devices, however, record only the number of particles with a range exceeding a certain amount $R$. Obviously, the probability of finding a range larger than $R$ is (Figure 19.3, curve *b*)

$$P(R) = \int_R^\infty p(R')dR' = \frac{1}{2} - \frac{1}{2}\Phi(\alpha[R - R_0]) \tag{19.8}$$

with $\Phi$ the error integral. The mean range $R_0$ is characterized by $P = 0.5$. Figure 19.4 gives the mean range of alpha particles, protons,

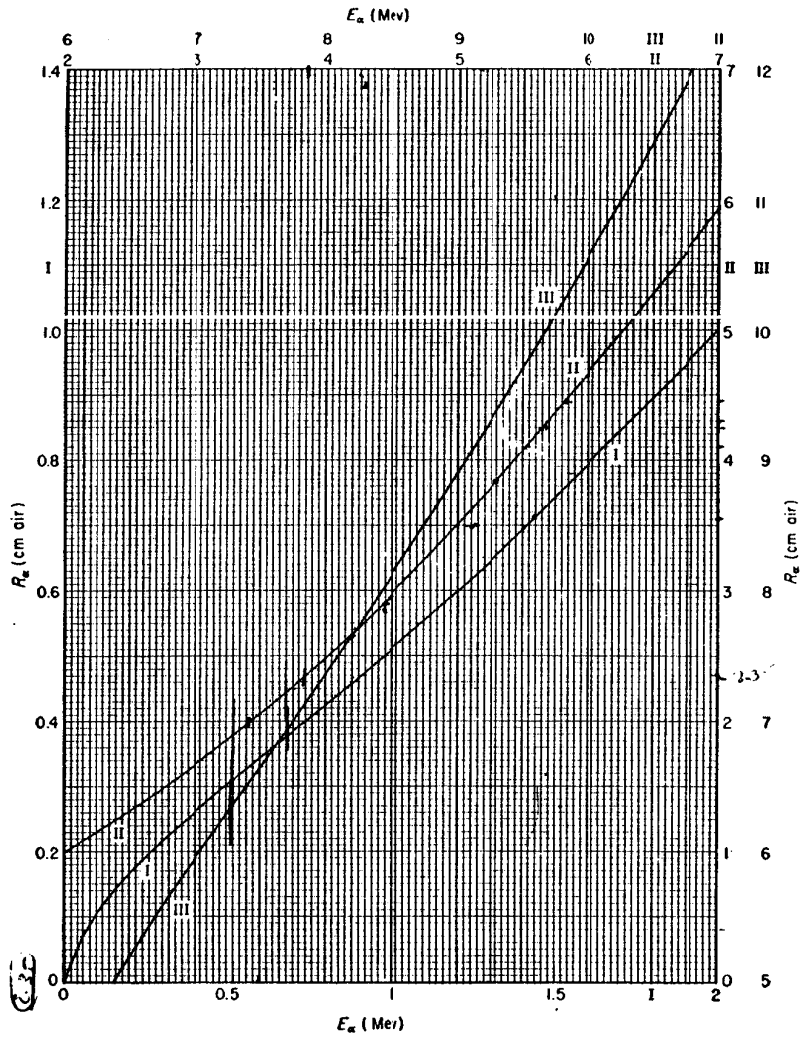


Fig. 19.4. (a) Mean range of alpha particles in dry air of 15° C and 760 mm Hg.[2]

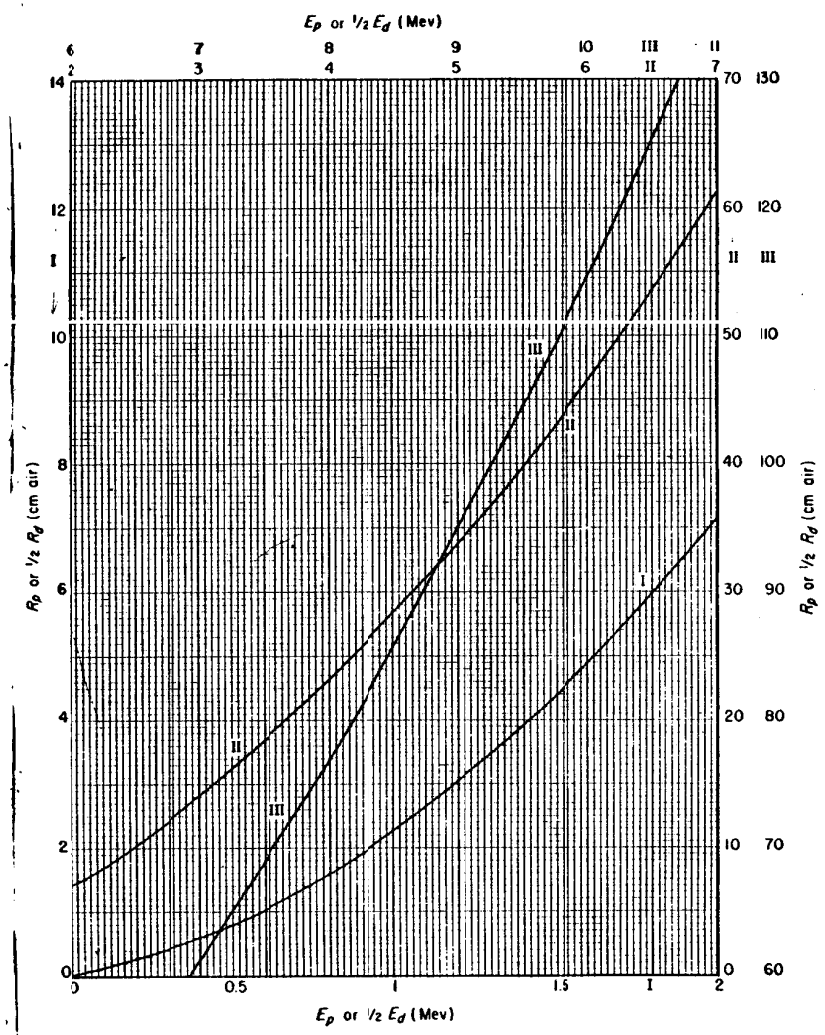


Fig. 19.4. (b) Mean range of protons and deuterons in dry air of 15° C and 760 mm Hg.[2]

and deuterons as a function of their energy, in dry air of 15° C, 760 mm Hg pressure.

*EXTRAPOLATED RANGE*

If the source is not infinitely thin, the apparent mean range (50% transmission) has no significance because the particles from deeper layers in the source have a shorter range. It is preferable, in this case, to

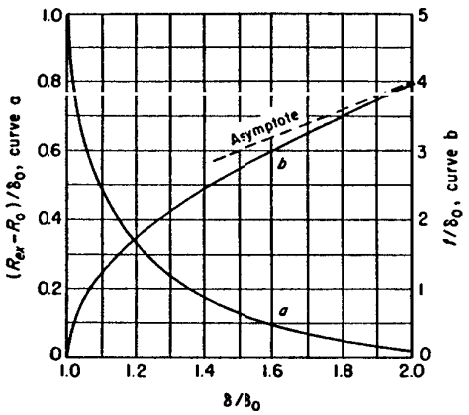


**Fig. 19.5. Calculation of mean range $R_0$ and source thickness $t$. $\delta$ = difference between the extrapolated range $R_{ex}$ and the half-intensity distance $R_{1/2}$. $\delta_0$ = same for thin source (cf. Fig. 19.3, values given in text).**

determine the so-called extrapolated range $R_{ex}$ by drawing the line of steepest tangent to the number-range curve. For thin sources the difference between the mean range and the extrapolated range can be calculated easily from equation 19.8 with the aid of Figure 19.3, curve *b*:

$$\delta_0 = R_{ex} - R_0 = \frac{P(R_0)}{-dP/dR} = \frac{\sqrt{\pi}}{2\alpha} \qquad (19.9)$$

The percentage difference $\frac{\delta_0}{R_0}$ decreases slowly with energy, being about 1.2% at 4 Mev, 1.1% at 8 Mev, 1% at 16 Mev.[1] For a target of thickness $t$, the range of 50% transmission, $R_{1/2}$, is by an amount $\frac{t}{2}$ shorter than the true mean range $R_0$. The extrapolated range is also slightly smaller than for a thin source. From the measurement of $\delta = R_{ex} - R_{1/2}$ and the knowledge of $\delta_0$ (1% to 1.2% of $R_0$), it is possible to calculate the true mean range $R_0$ with the aid of Figure 19.5.



## STOPPING POWER OF OTHER SUBSTANCES

The energy loss of alpha particles in substances other than air can be characterized in different ways.

*EQUIVALENT THICKNESS*

The equivalent thickness is that amount of material, customarily given in mg/cm², in which the particle loses the same amount of energy as in 1 cm of air. Values for a few elements are given in Table 19.1[1] (data by Rosenblum).

*Table 19.1*

Thicknesses Equivalent to 1 cm Air for Alpha Particles of about 6 Mev

| *Substance* | $t_{eq}$ *in mg/cm²* |
|---|---|
| mica | 1.43 |
| Al | 1.51 |
| Cu | 2.09 |
| Ag | 2.71 |
| Au | 3.74 |

*RELATIVE ATOMIC STOPPING POWER*

The relative atomic stopping power $s$ is the ratio of the energy losses per atom encountered in the substance and in air. According to equations 19.1, 19.2,

$$s = \frac{B}{B_{air}} \cong \frac{Z}{Z_{air}} \frac{\ln (2mv^2/I)}{\ln (2mv^2/I_{air})} \qquad (19.10)$$

with $s$ increasing somewhat less rapidly than $Z$ because the logarithmic term is diminished by the increase of the average excitation potential $I$ with $Z$.

*RELATIVE ELECTRONIC STOPPING POWER*

The energy loss per electron—relative to air—is given by

$$s_e = s \frac{Z_{air}}{Z} \cong \frac{\ln (2mv^2/I)}{\ln (2mv^2/I_{air})} \qquad (19.11)$$

Experimental values are given in Figure 19.6 for alpha particles of 4.66 Mev (Mano[4]) and about 31 Mev (Kelly[5]). In the more recent measurements, aluminum is chosen as the comparison substance rather than air, because aluminum absorber foils are more manageable than air absorption chambers. The factor $s_e(Z)$ depends approximately linearly on $\ln Z$. This is in qualitative agreement with equation 19.11 if it is assumed that $I$ is proportional to $Z$. One obtains, then,

EXPERIMENT **23** *Radiations of $Cu^{64}$ ($Zn^{65}$)*

The complete investigation of the decay of a radioactive isotope involves measurement of $\beta^-$ and $\beta^+$ spectra, gamma rays, and conversion lines; determination of the electron capture probability; coincidence measurements for the establishment of the decay scheme; measurement of angular correlations between different radiations and determination of the lifetime of the excited states for the assignment of quantum numbers to the various levels involved. Most of these measurements are beyond the limits of a laboratory course, requiring too elaborate measurement and evaluation techniques.

In the experiment, the radiations emitted by $Cu^{64}$ or $Zn^{65}$ are determined, using a crude beta-ray spectrometer, and $K$ capture is detected by the method of selective absorption.

## DECAY SCHEMES OF $Cu^{64}$ AND $Zn^{65}$

The best way to produce $Cu^{64}$ is irradiation of Cu with deuterons—$Cu^{63}(d,p)Cu^{64}$. Strong sources prepared by neutron capture can also be obtained from the United States Atomic Energy Commission, Oak Ridge, but the short half life of 12.9 hr makes this rather impractical. Since both neighbors, $Ni^{64}$ and $Zn^{64}$, are stable, dual decay is possible. The decay scheme is given in Figure 23.1. The intensity of the gamma radiation is small and not well known. It will be neglected in the experiment. Three modes of decay are possible. The total decay constant $\lambda$ is the sum of the partial decay constants $\lambda_{\beta^-}$, $\lambda_{\beta^+}$, $\lambda_c$. The branching ratios are approximately

$$\frac{\lambda_{\beta^-}}{\lambda} = 0.37 \qquad \text{for } \beta^- \text{ decay to } Zn^{64}$$

$$\frac{\lambda_{\beta^+}}{\lambda} = 0.18 \qquad \text{for } \beta^+ \text{ decay to } Ni^{64}$$

$$\frac{\lambda_c}{\lambda} = 0.45 \qquad \text{for electron capture to } Ni^{64}$$

The isotope $Zn^{65}$ is produced by the reactions $Cu^{65}(d,2n)Zn^{65}$, $Cu^{65}(p,n)Zn^{65}$, or by neutron capture from $Zn^{64}$. Because of the long

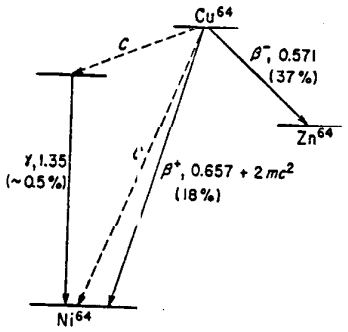


Fig. 23.1. Decay scheme of $Cu^{64}$. Vertical distances: differences of atomic masses.

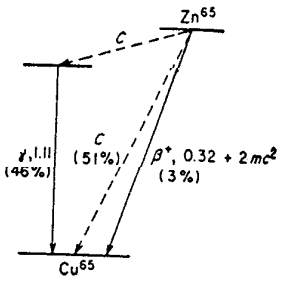


Fig. 23.2. Decay scheme of $Zn^{65}$.

half life of 250 days, it is a very convenient source for laboratory purposes, obtainable from the United States Atomic Energy Commission. Like all odd $A$ radioisotopes, $Zn^{65}$ decays only in one direction, into $Cu^{65}$ by $\beta^+$ emission or electron capture. The decay scheme is shown in Figure 23.2. In addition to positrons, gamma rays and X rays are emitted.

Furthermore, one always observes a distribution of Compton electrons produced by the gamma rays in the source and the backing unless extreme precautions are taken. The same effect occurs, obviously, with $Cu^{64}$, but it is unimportant there because of the low intensity of the gamma radiation.

## CHARGED PARTICLE SPECTRA

### *DETERMINATION OF THE ENERGY DISTRIBUTION*

The sign and the energy distribution of the charged particles emitted by the source are determined with the aid of a semicircular spectrometer.

Figure 23.3 shows a setup suitable for a crude experiment. The baffle system shown is brought between the pole pieces of a small electromagnet, making it necessary for the beta-particles to describe semicircular trajectories in order to reach the counter. For an electron of

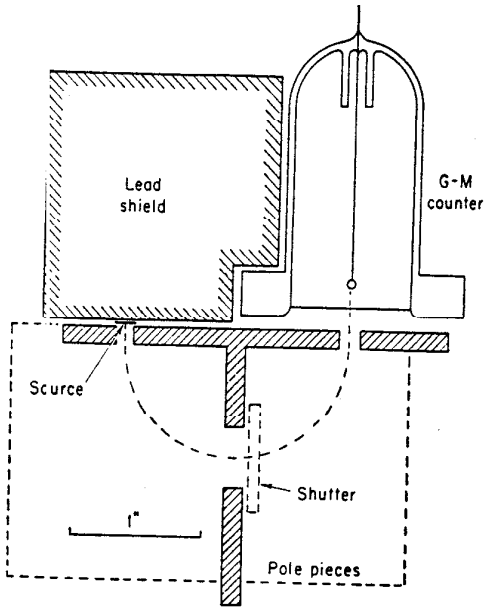


Fig. 23.3. Beta-ray "spectrometer."

momentum $p = mv$, the radius $\rho$ of the path in a magnetic field perpendicular to the direction of motion is given by

$$\frac{mv^2}{\rho} = \frac{evH}{c} \tag{23.1}$$

$$H\rho = \frac{cp}{e} \tag{23.2}$$

with $H\rho$ called the "magnetic rigidity" and measured in gauss-cm. (Note the inconsistency in symbol and unit, which is due to tradition. The symbol $B\rho$ or else the unit oersted-cm would be preferable.) The momentum, measured in units of $mc$, is

$$P = \frac{p}{mc} = \frac{eH\rho}{mc^2} = \frac{H\rho}{1{,}704} \tag{23.3}$$

The total energy, in units of $mc^2$, is

$$W = \frac{E}{mc^2} = \sqrt{P^2 + 1} = \sqrt{\left(\frac{H\rho}{1{,}704}\right)^2 + 1} \tag{23.4}$$

This is the most useful formula for obtaining the energy from $H\rho$. The kinetic energy, then, is simply

$$E_{\text{kin}} = mc^2(W - 1) = 0.511(W - 1) \text{ (Mev)} \tag{23.5}$$

The spectral distribution may be given by the number $N(W)dW$ of electrons with energies between $W$ and $W + dW$, or by the number $N(H\rho)dH\rho$ with $H\rho$ values between $H\rho$ and $H\rho + dH\rho$. Since the same number of particles is expressed as $N(W)dW$ and $N(H\rho)dH\rho$, one finds

$$N(W) = N(H\rho)\frac{dH\rho}{dW} = N(H\rho)\frac{W}{H\rho}(1{,}704)^2 \tag{23.6}$$

For a given field $H$ in the spectrograph, an intensity $I(H)$ is measured, proportional to the number of particles having radii of curvature between certain limits $\rho - \frac{\Delta\rho}{2}$ and $\rho + \frac{\Delta\rho}{2}$.

$$I(H) = \text{const } N(H\rho)\Delta(H\rho) = \text{const } N(H\rho)H\rho\frac{\Delta\rho}{\rho} \tag{23.7}$$

Since $\frac{\rho}{\Delta\rho}$, the resolving power of the instrument, is constant, the distributions can be calculated from the measured intensity by the formulas

$$N(H\rho) = \text{const}\frac{I(H)}{H\rho} \tag{23.8}$$

$$N(W) = \text{const}\frac{I(H)W}{(H\rho)^2} \tag{23.9}$$

*THEORETICAL SHAPE OF THE BETA SPECTRA*[1]

According to the Fermi theory, the shape of an allowed spectrum—i.e., for cases where the spin of the nucleus changes by not more than $1\hbar$, with conservation of parity—is given by the formula

$$N(W) = \text{const } PW(W_0 - W)^2F(Z,W) \tag{23.10}$$

The distribution is determined principally by the so-called statistical factor $PW(W_0 - W)^2$, which is proportional to the density of final states for an electron of energy $W$ and a neutrino of energy $W_0 - W$. Since it is low if the momentum of one of the particles is small, the intensity

drops to zero both near $W = 1$ and $W = W_0$. The factor $F(Z,W)$ gives the influence of the Coulomb field on the wave function of the electrons at the nucleus and therefore on the decay probability which depends essentially on the square of the wave function. For $Z = 0$, $F(Z,W) = 1$. It increases for $\beta^-$ particles with increasing nuclear charge and decreasing energy (attraction), whereas it decreases with $Z$ and decreasing energy for positrons (repulsion). Obviously $Z$ is the charge number of the *residual* nucleus in whose field the escaping beta particle moves. The shape of the distributions for different values of $Z$ is shown in Figure 23.4. Extensive graphs of $F(Z,W)$ have been given by Moszkowski.[2]

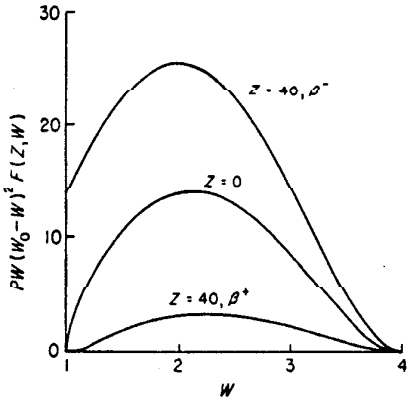


Fig. 23.4. Shape of allowed beta spectra for $W_0 = 4$ (maximum kinetic energy: 1.53 Mev) and $Z = 40$, 0, and "$-40$" (i.e., positron emission).

*FERMI-KURIE PLOT*

The direct determination of the upper limit $W_0$ of the spectrum is rather difficult because the intensity goes quadratically to zero near $W_0$. If one plots, however,

$$y = \left[\frac{N(W)}{WPF(Z,W)}\right]^{1/2} \tag{23.11}$$

as a function of $W$, one should get a straight line,

$$y = \text{const}\ (W_0 - W) \tag{23.12}$$

intersecting the abscissa at $W = W_0$ (Figure 23.5). This plot is called the Kurie plot after F. N. D. Kurie, who first developed the method, or the Fermi plot after E. Fermi, who is responsible for the theory. In addition to allowing an accurate determination of the upper limit, it provides a good check on the shape of the distribution. A deviation from formula 23.10 would reveal itself in a curvature of the plot.

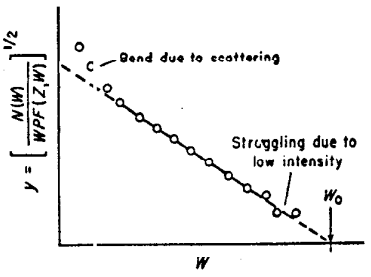


Fig. 23.5. Typical Fermi-Kurie plot.

Since for a spectrometer measurement $N(W)$ is given by the equation 23.9, the ordinate of the Fermi plot is

$$y = \left[\frac{I(H)}{(H\rho)^3 F(Z,W)}\right]^{1/2} \tag{23.13}$$

It is obviously permissible to omit any constant factor, e.g., the factor $\rho^3$ in the denominator, and to use

$$y = \left[\frac{I(H)}{H^3 F(Z,W)}\right]^{1/2} \tag{23.14}$$

*INTENSITIES*

The relative intensities of the $\beta^-$ and the $\beta^+$ spectra are obtained by plotting $N(H\rho) = \dfrac{I(H)}{H\rho}$ vs. $H\rho$ and integrating, for example, using a planimeter.

## ELECTRON CAPTURE

*IDENTIFICATION OF K CAPTURE*

During the process of $K$ capture no detectable radiation is emitted, since the energy is carried away by a neutrino. The hole left in the $K$ shell, however, will be filled by an electron from an outer shell, preferentially the $L$ shell. In a certain fraction of cases—given by the so-called fluorescence yield, $Y$—the transition energy is emitted in the form of a $K$-X ray characteristic of the daughter element. In the other cases it is used for the ejection of another electron (Auger electron) from one of the outer shells, no $K$ radiation being emitted. The fluorescence yield $Y$ increases strongly with increasing atomic number (Figure 23.6).

$K$ capture can be recognized and measured, therefore, by observing either Auger electrons or $K$-X rays (making sure that they do not follow internal conversion). Since the Auger electrons emitted by Ni have

energies of less than 10 kev, they are difficult to observe except in gases. The nature of the X rays, on the other hand, can be determined easily with the method of critical absorption. Table 23.1 lists the absorption coefficients of different materials for the $K$-X rays of Ni, Cu, and Zn. Since the absorption is mainly due to photoeffect, it drops suddenly,

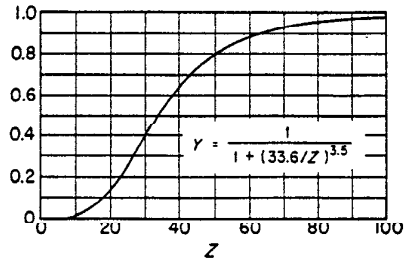


Fig. 23.6. Fluorescence yield.[3]

when, with increasing $Z$ of the absorber, the binding energy of the $K$ shell increases beyond the energy of the X ray in question. Thus the Cu $K$ radiation ($h\nu$ = 8.1 kev) is able to eject a $K$ electron from Fe and Co ($E_K$ = 7.1 and 7.7 kev), but not from Ni ($E_K$ = 8.3 kev). The mass absorption coefficient, therefore, drops sharply between Co and Ni.

*Table 23.1*

Mass Absorption Coefficients of $K$-X Rays,[4] in $cm^2/g$

| Emitter | Absorber | | | | | | |
|---|---|---|---|---|---|---|---|
| | H | C | A | Fe | Co | Ni | Cu |
| Ni | 0.5 | 5.5 | 144 | 400 | 54 | 58 | 61 |
| Cu | 0.5 | 4.5 | 116 | 328 | 358 | 48 | 51 |
| Zn | 0.5 | 3.7 | 93 | 270 | 290 | 310 | 41 |

*DETERMINATION OF THE INTENSITY OF THE K RADIATION*

A rough determination of the intensity of the X radiation is possible if the solid angle and the sensitivity of the counter are known. The probability that a photon hitting the counter will be counted is essentially given by the probability that it will be absorbed in the gas, within the sensitive volume. In contrast to gamma rays, the emission of secondary electrons from the walls is unimportant because of their extremely short range. For an end window counter, with the source

at a distance $d$ from the window (Figure 23.7), one obtains for the counting rate $n_x$

$$n_x = D_x \frac{1}{4\pi} \int_0^{\alpha} 2\pi \sin\theta(1 - e^{-\mu s(\theta)})d\theta \tag{23.15}$$

with $D_x$ the number of X rays emitted by the source, $\mu$ the absorption coefficient in the gas. The absorption in air and in the counter window

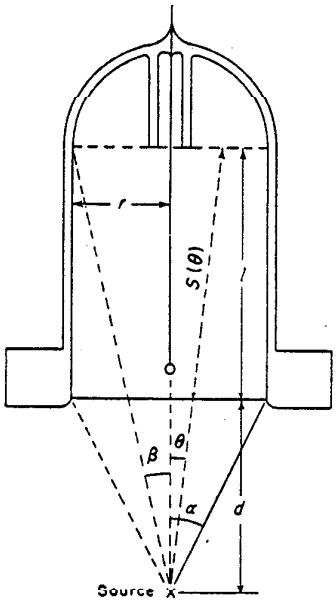


Fig. 23.7 X-ray sensitivity of end window counter. It is assumed that the length of the sensitive volume is given by the distance $l$ between the (plane) window and the end of the anode shield.

is neglected in 23.15. Generally, 23.15 must be evaluated graphically or numerically. If $\mu l \ll 1$, expansion of the exponential yields

$$n_x = D_x \frac{1}{2} \int_0^{\alpha} \mu s(\theta) \sin\theta d\theta \tag{23.16}$$

with the result

$$n_x = \frac{D_x \mu l}{2}\left[\ln\left(\frac{1}{\cos\alpha}\right) - \frac{d}{l}\ln\left(\frac{\cos\beta}{\cos\alpha}\right) + \frac{r}{l}(\alpha - \beta)\right] \tag{23.17}$$

For large source-counter distances, this is reduced to

$$n_x = D_x \mu l \frac{r^2}{4d(d + l)} \tag{23.18}$$

Under the same conditions one obtains for beta particles

$$n_\beta = D_\beta \frac{r^2}{4d^2} \tag{23.19}$$

The relative sensitivity of the counter for X rays is therefore approximately

$$\epsilon_x = \mu l \frac{d}{d + l} \tag{23.20}$$

It is obvious that calculations of this kind give only an approximate indication of the strength of the X radiation. For precise determinations, the X-ray efficiency of the arrangement must be obtained by coincidence (X-$\gamma$, X-$\beta$, or X-conversion electron) measurements.

*L CAPTURE*

It is very difficult to detect $L$ capture because of the low energy of the $L$ radiation or the Auger electrons emitted. Theoretically, the ratio $\lambda_L/\lambda_K$ is essentially given by the ratio of the (wave mechanical) probabilities of finding an $L$ electron or a $K$ electron in the nucleus. In the region of $Z = 30$ one obtains

$$\frac{\lambda_L}{\lambda_K} \cong 0.1 \tag{23.21}$$

## EXPERIMENT A. $Cu^{64}$

### EQUIPMENT

1. Small electromagnet with pole pieces of at least 1½ in. by 2½ in. A field strength of 2,000 oersteds should be obtainable across a gap of 1 in. or more. The calibration curve, field vs. current (for the demagnetized magnet), should be provided.
2. Baffle system as shown in Figure 23.3.
3. End window counter and scaler.
4. Set of Cu absorbers allowing variation of the absorber thickness in steps of about 10 mg/cm² up to 100 mg/cm². Additional absorbers of 200 and 400 mg/cm².
5. Ni, Co, and Fe absorbers. Though it is desirable to have different thicknesses, the absorption coefficients can be determined using only one absorber of each element, which reduces the intensity to about 50%. The appropriate thicknesses needed are 15 mg/cm² of Ni, 15 mg/cm² of Co, and 2.5 mg/cm² of Fe. Ni foil is readily available. The Co and Fe absorbers may be prepared by soaking filter paper with $Co(NO_3)_2 \cdot 6H_2O$

and $Fe_2(SO_4)_3$. The absorption due to the low $Z$ material is determined with the aid of dummy filter papers.

6. $Cu^{64}$ source. A copper foil of 0.0001 in. to 0.0005 in. is bombarded with deuterons. In view of the crudeness of the experiment it is not necessary to prepare an extremely thin source. An activated strip of about 1 in. by $\frac{1}{8}$ in. is glued on a sample card. The $Zn^{63}$ produced from $Cu^{63}$ is allowed to decay for at least 5 hr ($T_{\frac{1}{2}}$ = 38 min). The intensity of the long-lived $Zn^{65}$ is negligible.

7. $UX_2$ source (from one of the earlier experiments).

## MEASUREMENTS

1. Using the arrangement of Figure 23.3, determine with the UX source which direction of the current focuses $\beta^-$ particles.

2. Remove the UX source. Bring the Cu source in position. Destroy the residual magnetism in the magnet. Measure the $\beta^-$ intensity, $I(H)$, increasing $H$ in steps of about 150 oersteds up to 2,000 oersteds (for a focusing radius of 1 in.). For 0, 1,000, and 2,000 oersteds obstruct the baffle opening with an absorber of at least 500 mg/cm² in order to determine the gamma background.

3. Demagnetize and repeat step 2 for the positrons.

4. Remove the baffle. Mount the source below the magnet (Figure 23.8).

5. Demagnetize. Measure the total intensity ($\beta^- + \beta^+ + X + \gamma$) without magnetic field.

6. Measure the intensity for $H$ = 500, 1,000, 1,500, and 2,000 oersteds. It should be constant above 1,000 oersteds, being due only to X and gamma rays.

7. With a sufficient field (no charged particles) take an absorption curve in Cu by placing the absorbers on top of the source. If they were inserted in front of the counter, the gamma-counting rate (mainly annihilation radiation) would increase because of the production of secondary electrons in the absorber.

8. Measure the intensities ($X + \gamma$) for the Ni, Co, Fe absorbers and the filter paper.

## EVALUATION AND REPORT

1. Subtract the counter background and correct all intensities measured to a common time ($T_{\frac{1}{2}}$ = 12.9 hr).

2. Subtract the gamma background from measurements 2 and 3.

Calculate and plot $N(H\rho) = \frac{I(H)}{H\rho}$ as a function of $H\rho$ for the $\beta^-$ and the $\beta^+$ spectrum. Estimate the upper limits (in gauss-cm and Mev).

3. Construct the Fermi-Kurie plots for a more accurate determination

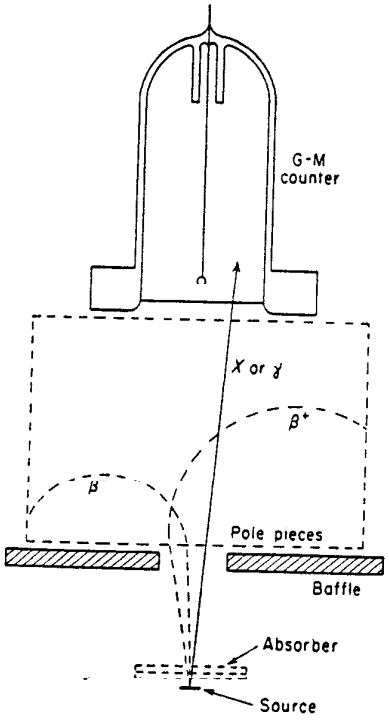


Fig. 23.8. Absorption of X rays.

of the maximum energies, using the values of $F(W,Z)$ given in Figure 23.9, and compare with Figure 23.1.

4. Integrate the distributions in order to find $\frac{D_{\beta^+}}{D_{\beta^-}} = \frac{\lambda_{\beta^+}}{\lambda_{\beta^-}}$.

5. Plot the Cu-absorption curve of the X and gamma radiation. Analyze it into the two components and calculate the mass absorption coefficient of Cu for the X rays.

6. Subtract the gamma intensity from the intensities found in measurement 3 with the other absorbers and calculate the mass absorption coefficients of Ni and paper. Use the latter to determine approximately the absorption due to the paper, the $NO_3^-$ and $SO_4^{--}$ groups, and the

water of crystallization in the Co filter, and calculate $\frac{\mu}{\rho}$ for Co and Fe. Compare all values with Table 23.1 and identify the nature of the X rays.

7. Calculate the ratio of the number of X rays to that of charged particles. Correct the X-ray counting rate for the absorption in the source (half the source thickness), the air, and the counter window, using

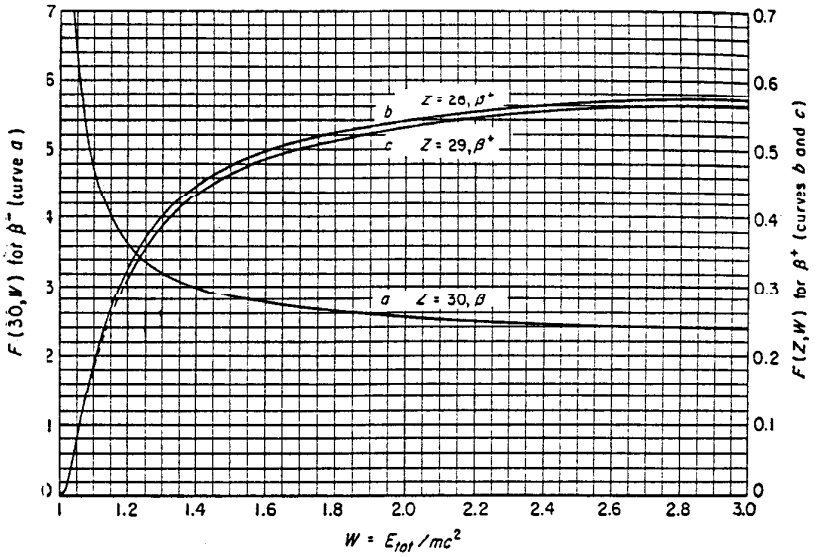


Fig. 23.9. $F(Z,W)$ for $\beta^-$ emission by Cu (a), $\beta^+$ emission by Cu (b), and $\beta^+$ emission by Zn (c).

the mass absorption coefficients found for Cu and paper. Correct similarly the $\beta^- + \beta^+$ counting rate (found in measurements 5 and 6 as the difference between the intensities for zero and high field) using an absorption coefficient of 25 cm²/g. (It could be determined by an additional absorption experiment.) The ratio $D_x/(D_{\beta^+} + D_{\beta^-})$ is equal to the ratio of the counting rates, divided by the relative efficiency $\epsilon_x$ for X-ray counting. Calculate $\epsilon_x$ according to equation 23.20 with the aid of Table 23.1.

8. Correct the number of X rays for the fluorescence yield (Figure 23.7) in order to obtain the $K$ capture probability and add 10% for $L$ capture. Give, as the final result, the branching ratios $\lambda_{\beta^-}/\lambda$, $\lambda_{\beta^+}/\lambda$, and $\lambda_c/\lambda$ and compare them with the accepted values (Figure 23.1).

## EXPERIMENT B. $Zn^{65}$

### EQUIPMENT

The same equipment is used except for a change of the Co absorber, which should contain only about 2.5 mg/cm² of Co. The source may be prepared by dissolving the bombarded Cu in a small quantity of nitric acid containing a few milligrams of ZnO as carrier—necessary only if very pure Cu is used. The material is evaporated to dryness and taken up in 0.5 *M* sulfuric acid. The Cu is removed by electrolysis onto a screen cathode of Cu or Pt. Use a current density of about 50 ma/cm² and stir rapidly. The Zn is precipitated as $ZnNH_4PO_4$. A mask is used over the filter paper in order to obtain a deposit on a strip of about 1 in. by ⅛ in. It is mounted in the usual way.

### MEASUREMENTS

The measurements are the same as for $Cu^{64}$.

### EVALUATION AND REPORT

The steps of the evaluation are identical with those for $Cu^{64}$ except for the following *changes:*

1. No correction for decay is necessary.
2. The negative particles are Compton electrons. Estimate the gamma energy from the upper limit of their distribution.
3. Construct the Fermi plot for the positrons only, using curve *c* of Figure 23.9.
4. Determine $\frac{D_{\beta^+}}{D_{e^-}}$. (This quantity has no significance but is needed for further evaluation.)
7. Calculate $\frac{D_x}{(D_{\beta^+} + D_{e^-})}$.
8. For $Zn^{65}$, $\lambda = \lambda_{\beta^+} + \lambda_c$. Give, as the final result, the branching ratios $\lambda_{\beta^+}/\lambda$ and $\lambda_c/\lambda$. Estimate the number of gamma rays emitted per electron capture, $\frac{D_\gamma}{D_c}$, using the gamma-ray sensitivity given in Figure 9.6 for brass counters. (This sensitivity will be slightly too high because of the thin window of the counter. This could be corrected by using the gamma-ray intensity obtained in an additional measurement with an absorber directly in front of the counter, in the arrangement of Figure 23.8.)

## REFERENCES

1. Konopinski, E. J., *Rev. Modern Phys.*, **15**, 209 (1943).
2. Moszkowski, S. A., "Research with the Chicago Cyclotron, Progress Report," August 1, 1949. See also graphs given by E. Bleuler and W. Zünti, *Helv. Phys. Acta*, **19**, 375 (1946) and a forthcoming publication by the United States National Bureau of Standards.
3. Steffen, R. M., O. Huber, and F. Humbel, *Helv. Phys. Acta*, **22**, 167 (1949).
4. Compton, A. H., and S. K. Allison, *X Rays in Theory and Experiment*. New York: D. Van Nostrand Company, 1935.